Tribology Letters (2021) 69:33
https://doi.org/10.1007/s11249-021-01405-1

ORIGINAL PAPER

Experimental Research on Sliding Friction of Dense Dry Particles Lubricated Between Parallel Plates

Fanjing Meng[1] · Huabo Liu[1] · Shaozhen Hua[1] · Minghua Pang[2]

Received: 28 November 2020 / Accepted: 1 February 2021 / Published online: 18 February 2021

Abstract

Particle flow lubrication is a promising choice for extreme working conditions. Lubricated by dense dry particles between parallel plates, clarifying the sliding friction characteristics are significant to the design and parameter selection of particle-lubricated warm forming die, which is not well studied yet through the experimental methods. A self-developed testing apparatus was used to study the sliding tribological characteristics of parallel plates under dense particle lubrication. The experimental results showed that the dry particle lubrication between parallel-plates behaves excellent lubrication characteristics on sliding friction. The average coefficient of friction between the upper palate and particles increases rapidly with the increase of pressure load while corresponding to the change of average coefficient of friction, the average friction force increases linearly with the increase of pressure load. The force chain line between the upper plate and the particle lubrication media becomes thicker with the increase of pressure load, indicating that the contact force and contact stress are increasing. The average coefficient of friction and average friction force decrease with the increase of sliding velocity. The force chain line between the upper plate and the particle lubrication media becomes thinner with the increase of the sliding velocity, indicating that the contact force and contact stress are decreasing. The greater the contact stress is, the greater the average coefficient of friction will be. This study provides a deep understanding of the sliding tribological behaviors of the warm-forming die lubricated by the particle media.

✉ Fanjing Meng
mengfanjing0901@126.com

[1] School of Mechanical Engineering, Henan Institute of Technology, Xinxiang 453003, Henan, China

[2] School of Mechanical and Electrical Engineering, Henan Institute of Science and Technology, Xinxiang 453003, Henan, China

Graphical Abstract

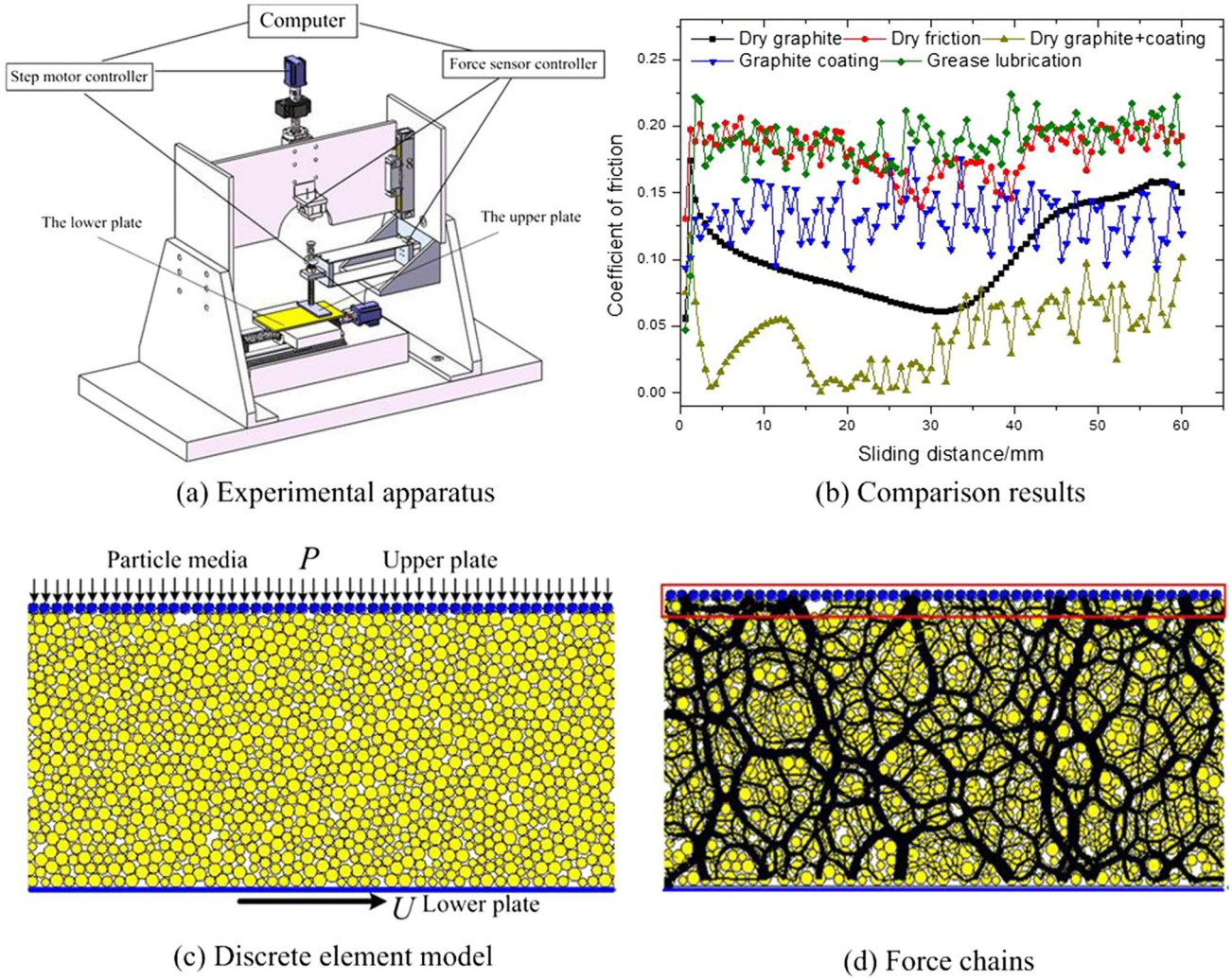

(a) Experimental apparatus

(b) Comparison results

(c) Discrete element model

(d) Force chains

Keyword Particle flow lubrication · Sliding friction · Force chains · Contact force · Warm forming die

1 Introduction

For the friction pairs, adding suitable lubricating media is one of the key technologies to ensure their safe, reliable and efficient operation. With the development of industry and aerospace technology, extreme working conditions such as high temperature, high vacuum and so on have emerged [1–4]. Therefore, in the field of lubrication, it is necessary to constantly find new lubrication methods to meet the requirements of these extreme working conditions. Wornyoh et al. [5] believed that dry particulate matter can be used as an effective material for lubrication under extreme working conditions (i.e., high temperature and/or high load), where the traditional lubricants could not play the role of lubrication. For example, an increase in the capacity of turbine engines would produce a high temperature of more than the order of 800 °C inside the engine. In the warm forming die manufacturing process, high temperature and high-pressure conditions were also inevitable [6]. At the temperature was higher than 500 °C or under high loads, the traditional liquid lubricants could not bear the loads, therefore, a new technology of solid/particle lubrication was used.

The particle flow lubrication is to use solid particles as lubrication media to reduce the contact between two surfaces in relative motion by using the contact, friction, collision and extrusion of particles in the friction gap, so as to protect the surface from damage [7–9]. It has good environmental adaptability and can carry static load [10]. It overcomes the problems of poor adaptability of liquid

Fig. 1 The photographs of the experimental materials. **a** The upper and lower plates, and **b** graphite particle lubrication media

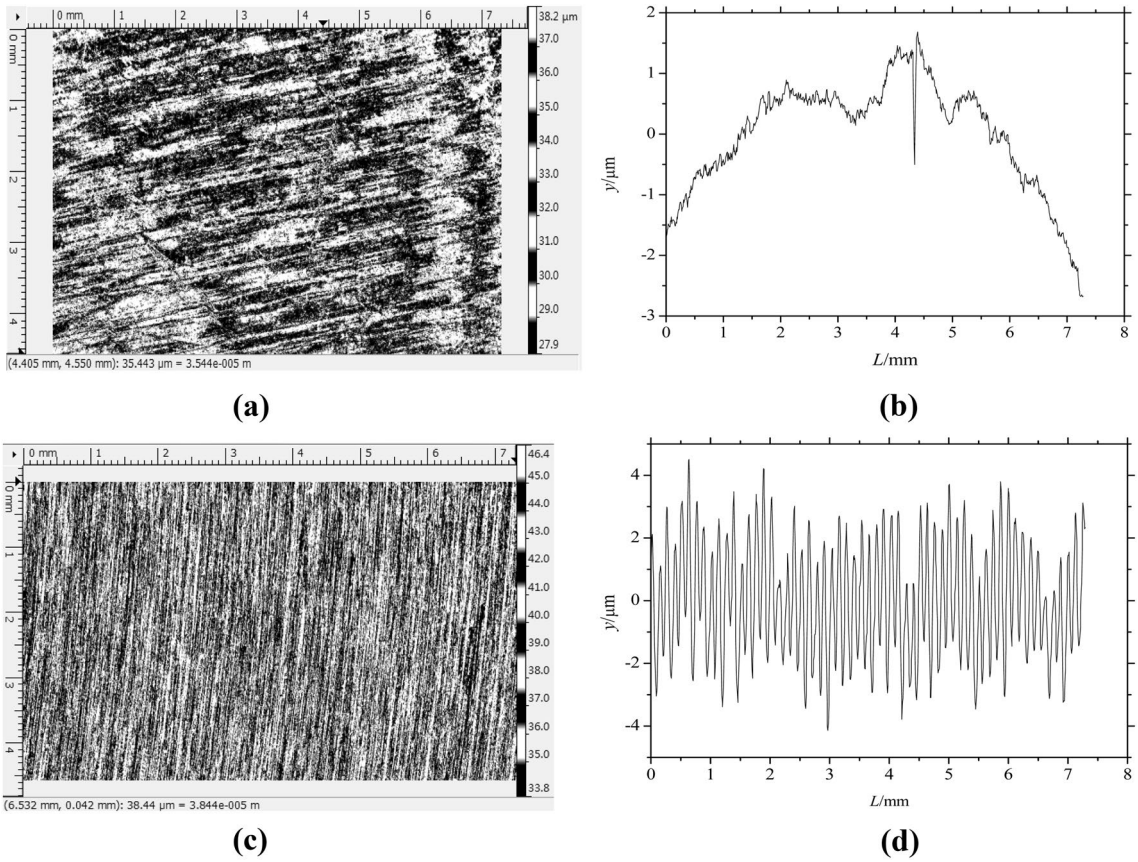

Fig. 2 The upper and lower plates used in this study. **a** Surface topography of the upper plate, **b** the height value indicated by the surface roughness of the upper plate, **c** surface topography of the lower plate, and **d** the height value indicated by the surface roughness of the lower plate

lubrication temperature, limited wear life of solid lubrication coating and bonding strength of the solid coating. At the same time, the particle system also has the characteristics of dissipation and the influence of temperature on the movement of the system can be ignored [11]. Therefore, particle flow lubrication is especially suitable for some special working conditions, such as space field [12]. It is a brand-new, innovative and challenging work to study the phenomena, laws and characteristics of particle flow lubrication and the influence of particle characteristics on lubrication [13, 14]. It is of great significance if we can establish the theory and method of particle flow lubrication which can give full attention to the characteristics of particulate matter and guide the application through systematic tribological research.

In the field of tribology, based on the multi-body interaction theory [15], particle flow lubrication has attracted scholar's attention, and some research attempts have been carried out. Heshmat and Brewe [16, 17] carried out a particle flow

lubrication experiments for the first time by adding titanium dioxide powder into thrust bearing; their results showed that a familiar hydrodynamic pressure curve could be generated by the particle flow lubrication method, and an empirical hydrodynamics theoretical model was established. Elkholy et al. [18, 19] used the stainless steel ball with a diameter of about 3 mm as particle lubrication media to study the shear expansion and stick–slip motion of particles; their results showed that the stick–slip occurred when particles inside granular materials began to roll and slid at the same time. The force of each particle was uneven, and the external force was supported by the force chain structure formed between the particles. When the force chain became unstable, the spatial position of some particles would change, so the force acting on some particles decreased sharply, and the decrease of the force directly leaded to the sharp decrease of the internal stress of the granular material. Rao et al. [20, 21] used a "Rambaudi CNC milling machine" to study the role of the solid lubricants on the surface roughness, specific energy and cutting forces while grinding SiC as well as AISI 1045 steel materials; the purpose of their study was to improve the surface roughness and the dimensional accuracy of products in ending milling. Iordanoff et al. [22] designed and developed an experimental apparatus to study the granular flow regimes between two parallel plates that lubricated by the granular media; further, the pressure load, the restitution coefficient as well as the shear velocity were considered in the experiments to reveal the influence of these input parameters on their dynamic behaviors. Kinura et al. [23] analyzed the lubricating and insulating ability influenced by the components of powder lubricants; their results showed that the composition change of the powder lubricants had a significant effect on the ejection force of the ejector pin in the die casting. Recently, Wang et al. [24–27] used the DEM and the FEM-DEM coupling method to explore the nonlinear phenomena, force chains in the frictional interface, multi-scale mechanical characteristics, and the startup dynamic process of the friction pairs lubricated by granular media; their research results further clarified the dynamic characteristics of particle flow lubrication and provided the corresponding basis for the application of particle flow lubrication.

Solid particle lubrication media itself is a discrete body, which has the characteristics of discontinuity and anisotropy [28]. Particle flow lubrication system is a complex and enormous system with many unique dynamic behaviors [29]. Many scholars have studied the characteristics of particle flow lubrication through theoretical and numerical methods from different aspects. However, the related research works through the experimental methods are still very lacking, which leads to the failure to fully understand the tribological characteristics of particle flow lubrication, and also hinders the application and promotion of this technology in the industry. In this study, a self-developed experimental device was used to study the sliding tribological characteristics of parallel plates under dense particle lubrication, the friction behaviors of particle flow lubrication was observed under the influence of the pressure load as well as the sliding velocity, aiming to provide the basis for the application of particle flow lubrication. The rest of this study is arranged as follows. Section 2 briefly introduces the material properties and the experimental apparatus. Section 3 is composed of three parts: part 1 is the comparative study of particle flow

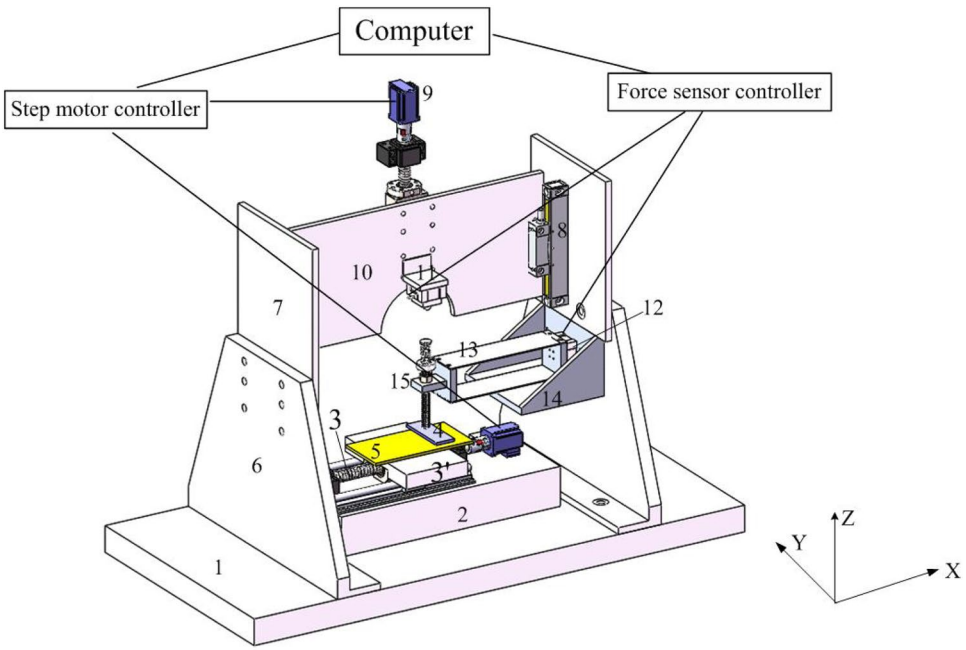

Fig. 3 Three-dimensional schematic diagram of this experimental apparatus: 1-Base of apparatus; 2-Ball screw connecting seat; 3-Ball screw; 3′-Moving platform; 4-Upper plate; 5-Lower plate; 6-Side column; 7-Grating ruler connecting plate; 8-Grating ruler; 9-Rotary stepper motor; 10-Z-direction sensor connecting plate; 11-Z-direction pressure sensor; 12-X-direction tension pressure sensor; 13-Cantilever beam; 14-Sensor fixed base; 15-Upper plate clamp (gland is arranged from top to bottom on the screw, spring and adjusting nut)

Table 1 The meaning of all lubrication methods

Lubrication methods	Lubricant	Weight (g)
Grease lubrication	Grease	2.135
Dry friction	No lubricant	0
Dry graphite lubrication	Dry graphite powder	3.825
Graphite coating lubrication	Dry film lubricant-graphite	1.723
Graphite coating + dry graphite lubrication	Film lubricant, and dry graphite powder	1.723, 3.825

lubrication with the other typical lubrication methods, part 2 observe the influence of pressure load on sliding friction, the influence of sliding velocity on sliding friction is analyzed in part 3. Section 4 summarizes this study.

2 Experimental

2.1 Material Properties of the Upper Plate, Lower Plate and Particle Lubrication Media

As shown in Fig. 1a, the upper plate was made of carbon steel, and the dimension of its contact surface was 40 × 20 mm. The material of the lower plate was H62 brass, and its dimension was 130 × 100 × 4 mm. The graphite powder used in this study was shown in Fig. 1b, with a weight of about 3.825 g. The diameter size of the graphite powder was about 25.6–38.4 μm, and its average diameter was about 30 μm. In this study, the diameter of graphite powder was measured by a GXL-202i Centrifugal Sedimentation Granulometer, which was based on Stokes theory of the sedimentation method. In the process of measurement, the sedimentation velocity of particles was proportional to the square of particle diameter.

As shown in Fig. 2, the roughness average (*Ra*) of the lower and upper plate was 737.100 nm and 1.51389 μm, respectively, which was measured by a RTEC-UP 3D profilometer. The length of the measuring line was defined as *L* and the height represented by the measured surface roughness was specified as *y*. The hardness of the upper plate was HRC52 measured by a Rockwell hardness tester

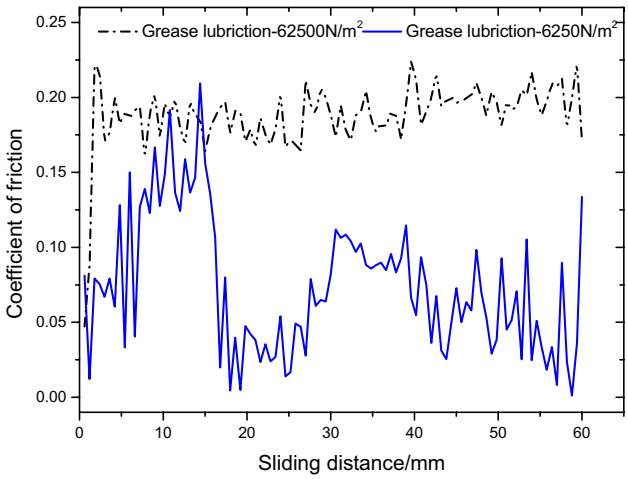

Fig. 5 Effect of pressure load on the coefficient of friction under grease lubrication

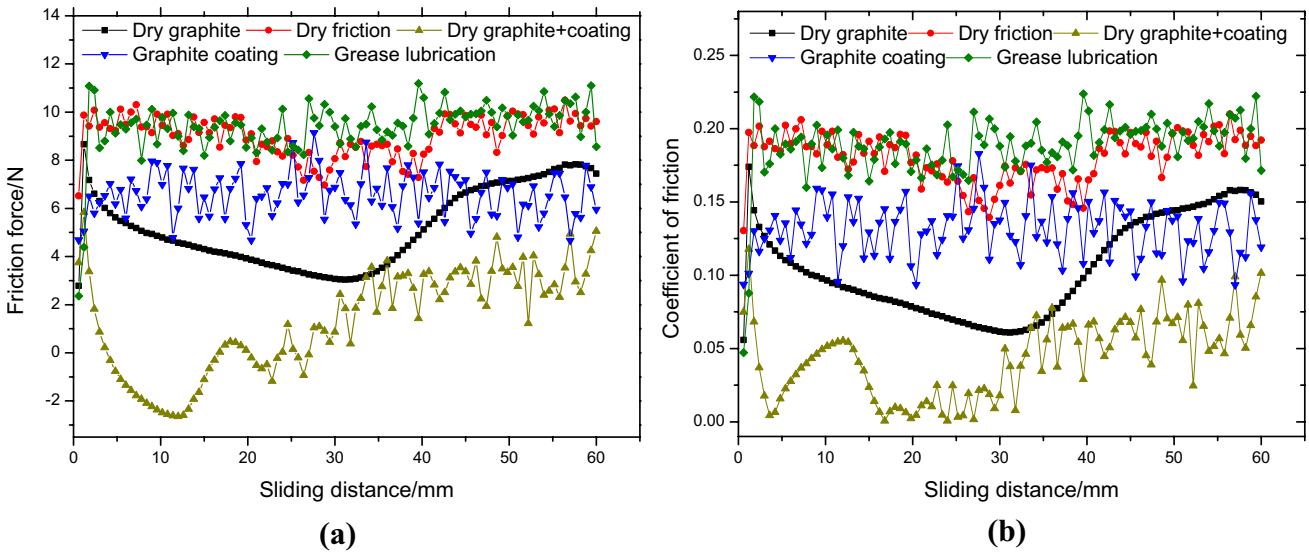

Fig. 4 The tribological characteristics of parallel plates with typical lubrication methods. **a** Variations of the friction forces, and **b** variations of the coefficients of friction

(Jitaike Instrument Hr-150a series), and the hardness of the lower plate was HV110 measured by a Vickers hardness tester (DECCA-HVS-100Z series). The elastic modulus of the upper and lower plates were 206 and 90 Gpa, respectively, measured by the microcomputer controlled electro hydraulic servo universal testing machine (WA-600KE series), and their Poisson's ratios were 0.26 and 0.34, respectively, measured by the force & strain comprehensive parameter tester (XL2118 series). Before the experiment, the upper and lower plates were cleaned with acetone. The graphite powder with the purity of 99.98%, density of 1.78 g/cm^3, elastic modulus of 9.8 GPa and Poisson's ratio of 0.301 were used in this study.

2.2 Experimental Apparatus

In order to study the sliding tribological characteristics of parallel plates under dense particle flow lubrication, an experimental system as shown in Fig. 3 was developed. Figure 3 was the three-dimensional schematic diagram of this experimental apparatus. A threaded hole was machined in the middle of the upper plate, which was connected with the screw in the upper plate clamp, and the height was adjusted by the screw and the adjusting nut arranged on the screw.

The moving platform was arranged above the ball screw, and the middle position of this moving platform was processed with a threaded hole. The lower plate was fixedly connected with this moving platform through the threaded hole and can move parallel along the Y direction of the

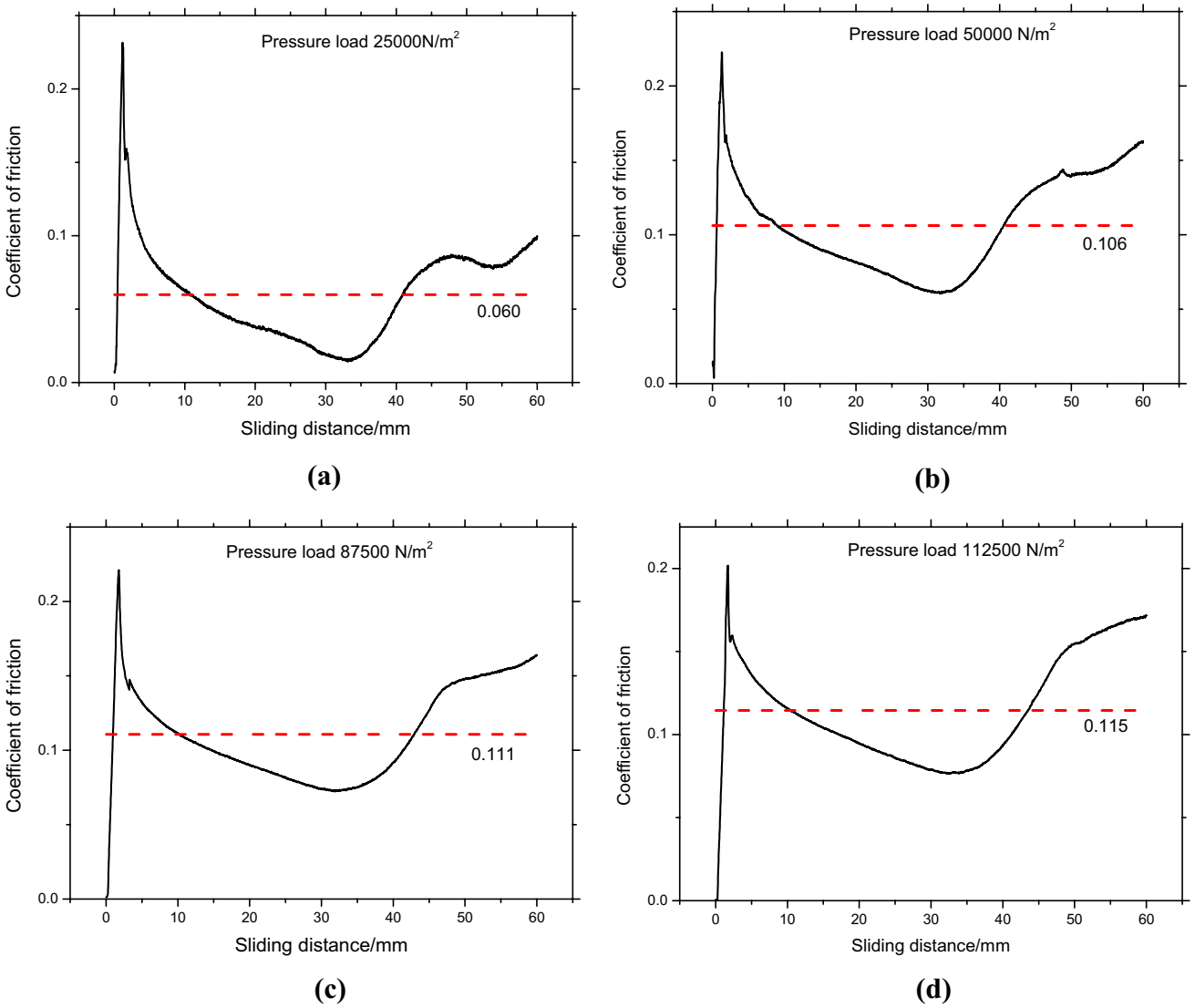

Fig. 6 Variation of the coefficient of friction with sliding distance under different pressure load. **a** 25,000 N/m^2, **b** 50,000 N/m^2, **c** 87,500 N/m^2, and **d** 112,500 N/m^2

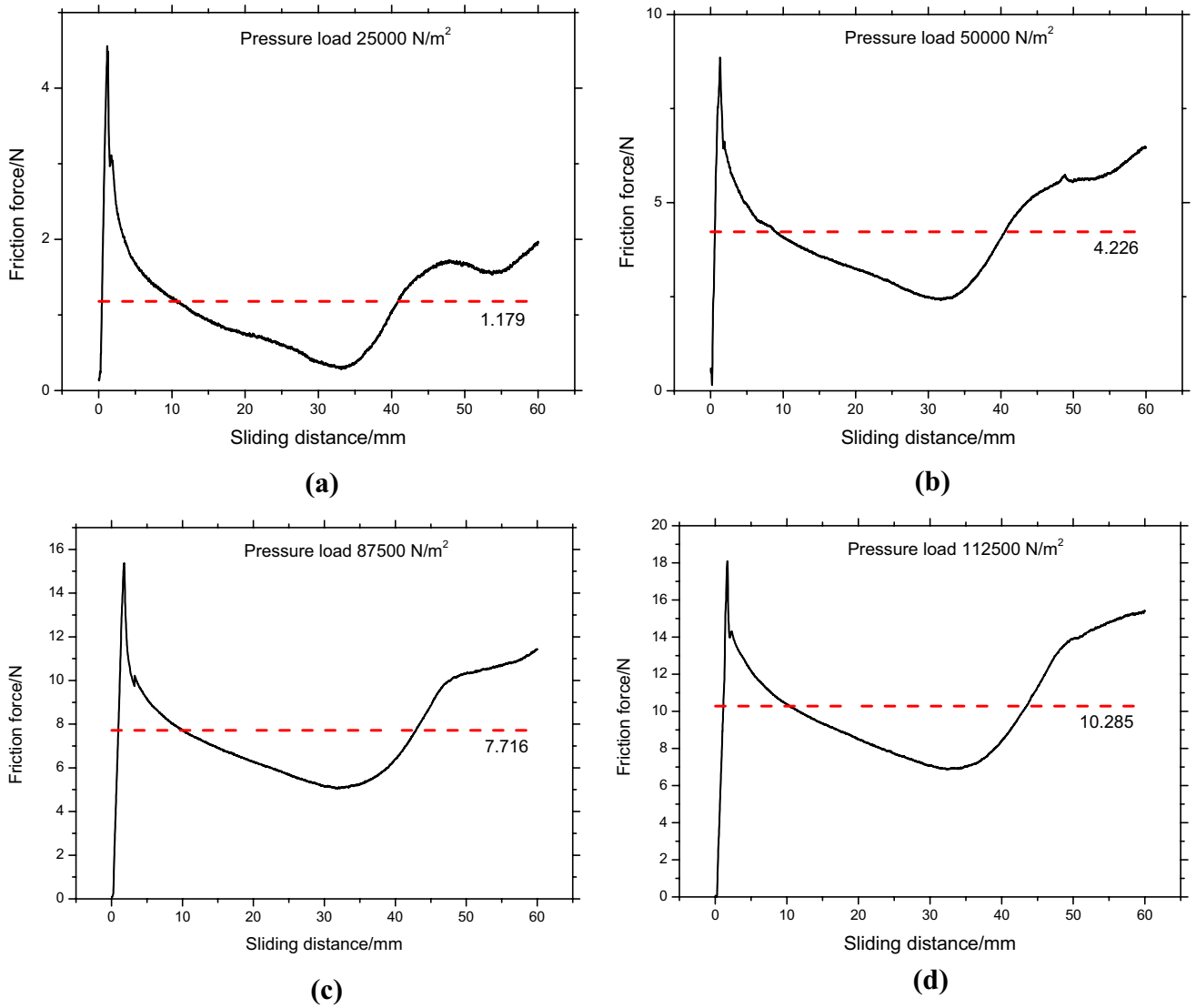

Fig. 7 Variation of the friction force with sliding distance under different pressure load. **a** 25,000 N/m^2, **b** 50,000 N/m^2, **c** 87,500 N/m^2, and **d** 112,500 N/m^2

coordinate axis driven by the ball screw, and the ball screw was driven by a rotary stepper motor. A spring and a gland were arranged on the top of the upper plate clamp, and a pressure sensor (RTEC Instruments, FZMA-200N-931) was arranged right above the gland to measure the positive pressure along the Z direction of the coordinate axis. This pressure sensor was connected with the Z-direction sensor connecting the plate. Before the experiment, driven by the rotary stepper motor and ball screw, this pressure sensor contacted with the gland and gradually pressed down to a set initial pressure value. A pressure sensor (RTEC Instruments, FXM-200N-ARM-934) was arranged on the right side column, which can measure the tension force along the X direction of the coordinate axis. The left side of this sensor was connected with a cantilever beam, and the end of this cantilever beam was connected with the upper plate clamp. The force measured by the Z-direction sensor was defined as the positive pressure F_Z, and the force measured by the X-direction sensor was defined as the friction force F_X. The coefficient of friction in the measurement process could be expressed as COF = F_X/F_Z.

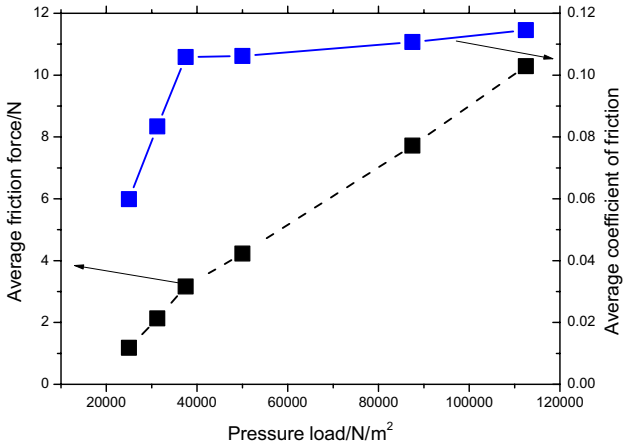

Fig. 8 Variation of the average coefficient of force and friction force with the pressure load

3 Results and Discussion

3.1 Comparative Study with Typical Lubrication Methods

In order to better understand the tribological characteristics of parallel plates under dense particle flow lubrication, the following comparative tests are carried out. The sliding velocity and pressure load are set as 2 mm/s and 62,500 N/m^2, respectively. The lubrication methods select in the comparative test included: dry friction, dry graphite, graphite coating, graphite coating + dry graphite and grease (Changcheng Shangbo General Grease, China) lubrication. The graphite coating materials use in this test included 10–20% propane, 10–20% butane, 40–50% heptane, < 2% toluene, 20–30% 2-propanol and < 2% graphite. The meaning of all lubrication methods are presented in Table 1.

At the same time, to ensure the accuracy of the comparison test results, the test under each lubrication condition is repeated for 10 times, and each data point in the graph is the average value of 10 measurement results. Figure 4a and b show the variation of friction force and the coefficient of friction with sliding distance.

The experimental results show that the tribological characteristics of graphite coating + dry graphite and dry graphite are better, the average friction force is 1.338 and 5.139 N, and the average coefficient of friction is 0.044 and 0.106, respectively.

The tribological characteristic of graphite coating is slightly worse than that of graphite lubrication, the average friction force and the average coefficient of friction is 6.517 N and 0.130, respectively. The tribological characteristic of dry friction is poor, the average friction and coefficient of friction increases to 8.944 N and 0.179, respectively. When the high pressure of 62,500 N/m^2 is applied to the

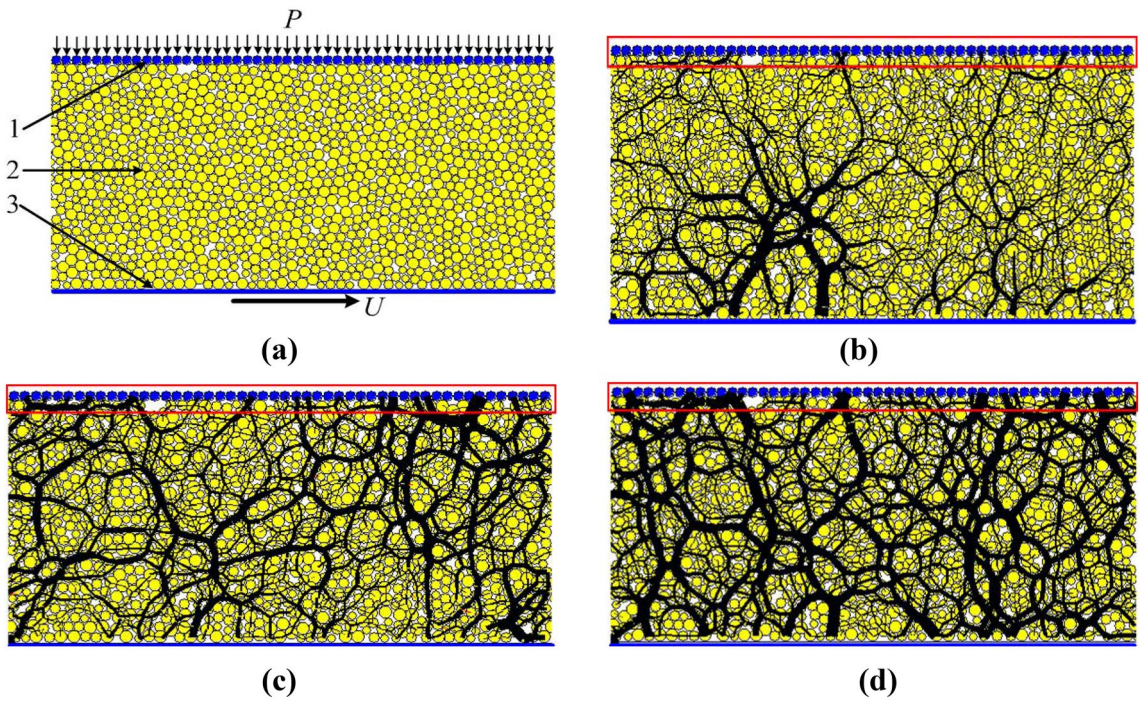

Fig. 9 Particle flow lubrication model and the graph of force chain network between upper plate and particle lubrication media under different pressure loads. **a** Discrete element model of the particle flow lubrication, **b** 25,000 N/m^2, **c** 50,000 N/m^2, and **d** 87500 N/m^2

upper plate and grease lubrication is used, the tribological test results are similar to those of dry friction, the average friction force and average coefficient of friction is 9.210 N and 0.183, respectively. The reason for this phenomenon is: in the process of high-pressure shear movement, the lubricating grease layer covering the lower plate breaks due to high pressure, which makes the upper and lower plates contact directly to form dry friction. Thus, the friction interface is operating under a boundary type regime, and this grease-lubricated case does not improve the performance. Beside, the viscosity of lubricating grease hinders the movement of the lower plate, which makes the measured average friction force and the average coefficient of friction slightly increase compared with dry friction. This can be explained by the comparison test results shown in Fig. 5.

As shown in Fig. 5, under the condition of applying low pressure of 6250 N/m^2 to the upper plate and adopting grease lubrication, a good lubricating oil film can be formed between the upper and lower plates, thus significantly reducing the average friction coefficient measured in the test. Moreover, the substantial increase in load will drastically destroy the lubrication layer and increase the interface friction.

3.2 Influence of Pressure Load on Sliding Friction

In this study, the coefficient of friction and friction force between the upper plate and the particle lubrication media are measured by a self-developed experimental apparatus. During the measurement, the sliding distance of the lower plate is 60 mm, the sliding velocity is 2 mm/s, and the pressure loads applied on the upper plate are 25,000, 31,250, 37,500, 50,000, 87,500 and 112,500 N/m^2, respectively. To ensure the accuracy of the measurement results, the test under the same pressure load condition is repeated for ten times, and each data point in the graph is the average value of the 10 measurement results. Figure 6 shows the variation law of coefficient of friction between upper plate and particle lubrication media under different pressure loading conditions. The average coefficient of friction is shown by dotted line, and its specific value is indicated on the right side of the figure. Figure 7 shows the variation law of friction force between the upper plate and particle lubrication media under different pressure load conditions during the sliding process of the lower plate. The average friction force in the figure is shown by a dotted line, and its value is also shown on the right side of the figure.

As shown in Figs. 6 and 7, the coefficient of friction and friction force increase rapidly to a certain peak value with the increase of sliding distance, and then gradually decrease, reaching a certain trough value when the sliding distance is about 33 mm. After that, the coefficient of friction and friction force increase with the increase of sliding distance. Under the pressure load of 25,000, 50,000, 87,500 and 112,500 N/m^2, the values of average coefficient of friction are 0.060, 0.106, 0.111 and 0.115, and the values of corresponding average friction force are 1.179, 4.226, 7.716 and 10.285 N, respectively.

Figure 8 shows the variation of the average coefficient of friction and average friction force with pressure load. As shown in Fig. 8, the average coefficient of friction increases rapidly with the increase of pressure load. When the pressure load is 37,500 N/m^2, the value of average coefficient of friction increases to 0.106, then, with the continuous increase of pressure load, the average coefficient of friction continues to increase, but the increase range becomes very small. Finally, the value of the average coefficient of friction remains at the level of 0.114. Corresponding to the change of average coefficient of friction, the average friction force increases linearly with the increase of pressure load. Those results show that the pressure load has a significant effect on the average coefficient of friction and the average friction force.

As shown in Fig. 6, the average coefficient of friction first increases rapidly with the increase of pressure load, and then the increasing trend becomes smooth. The reason for the variation of the average coefficient of friction is closely related to the measurement of the maximum contact stress between the upper plate and the single particle. The maximum contact stress can be calculated by Hertz theory [30], as shown in Eq. (1).

$$\sigma_{H\max} = \frac{1}{\pi}\sqrt{6F\left\{\frac{\frac{1}{\rho_1}+\frac{1}{\rho_2}}{\frac{1-\mu_1^2}{E_1}+\frac{1-\mu_2^2}{E_2}}\right\}^2} \quad (1)$$

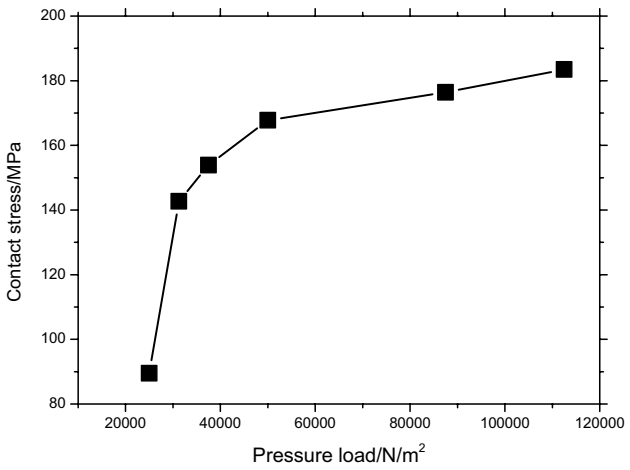

Fig. 10 Variation of contact stress with pressure load

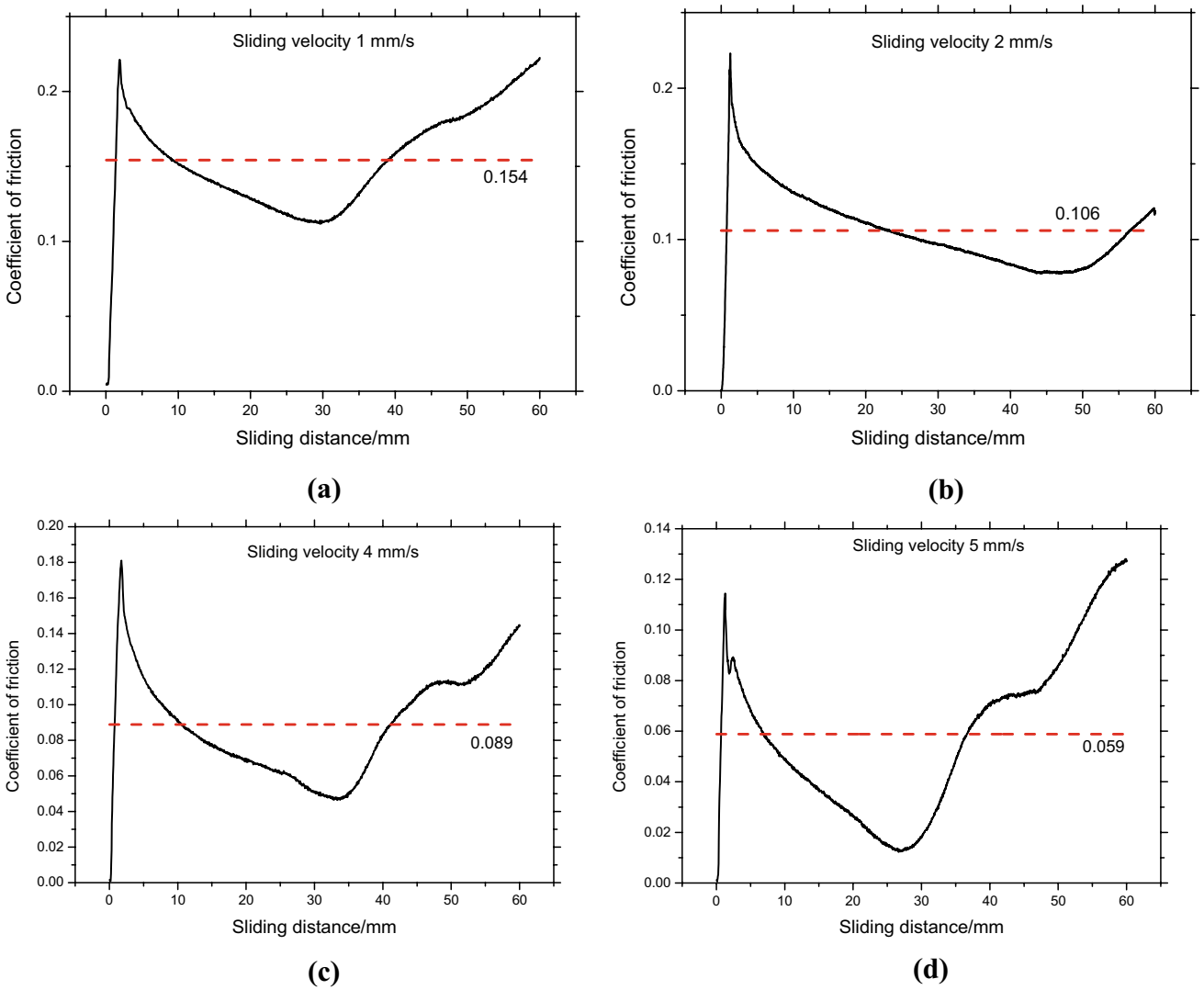

Fig. 11 Variation of the coefficient of friction with sliding distance under different sliding velocity. **a** 1 mm/s, **b** 2 mm/s, **c** 4 mm/s, and **d** 5 mm/s

where ρ_1 is the curvature radius parameter of the upper plate, and ρ_2 denotes the curvature radius parameter of the particle. The parameters of μ_1 and μ_2 denote Poisson's ratio of the upper plate and particle, respectively. The parameters of E_1 and E_2 denote the elastic modulus of the upper plate and particle. F is the pressure of contact zone between the upper plate and particle, and $\sigma_{H\max}$ is the maximum contact stress.

Meantime, the change of the maximum contact stress can be reflected by the force chain network [31, 32] as shown in Fig. 9. In the particle flow lubrication system, because the particle media is dispersed, the force of each particle media is not uniform. The contact force is formed by the contact between the particles, and the contact force forms a force chain with different strength, which plays a role in supporting the external force in the particle flow lubrication system. When the force chain becomes unstable, the spatial position of some particle media will change, hence, lift-off occurs [33]. The large noise event of particle lubricated bearing is also closely related to the stability of the force chain structure between particles. Through the action of a shear force, the force chain structure between particles is destroyed and a new force chain structure is constantly formed so that the internal stress of particles fluctuates. At early stages, the force chain structure between particles is not stable, the stress fluctuation range is large and frequent, and the noise is large. When the particle media can play a good role in the lubrication of the bearing, the force chain structure between the particle media is relatively stable, the stress fluctuation range is small, and the system becomes quiet [18, 19, 34, 35]. Figure 9a shows the numerical model established by the discrete element method (PFC2D commercial software).

The length L and height H of the numerical model are 1.6 and 0.8 mm, respectively. The particle lubrication media in the numerical model is composed of 1200 spherical particles

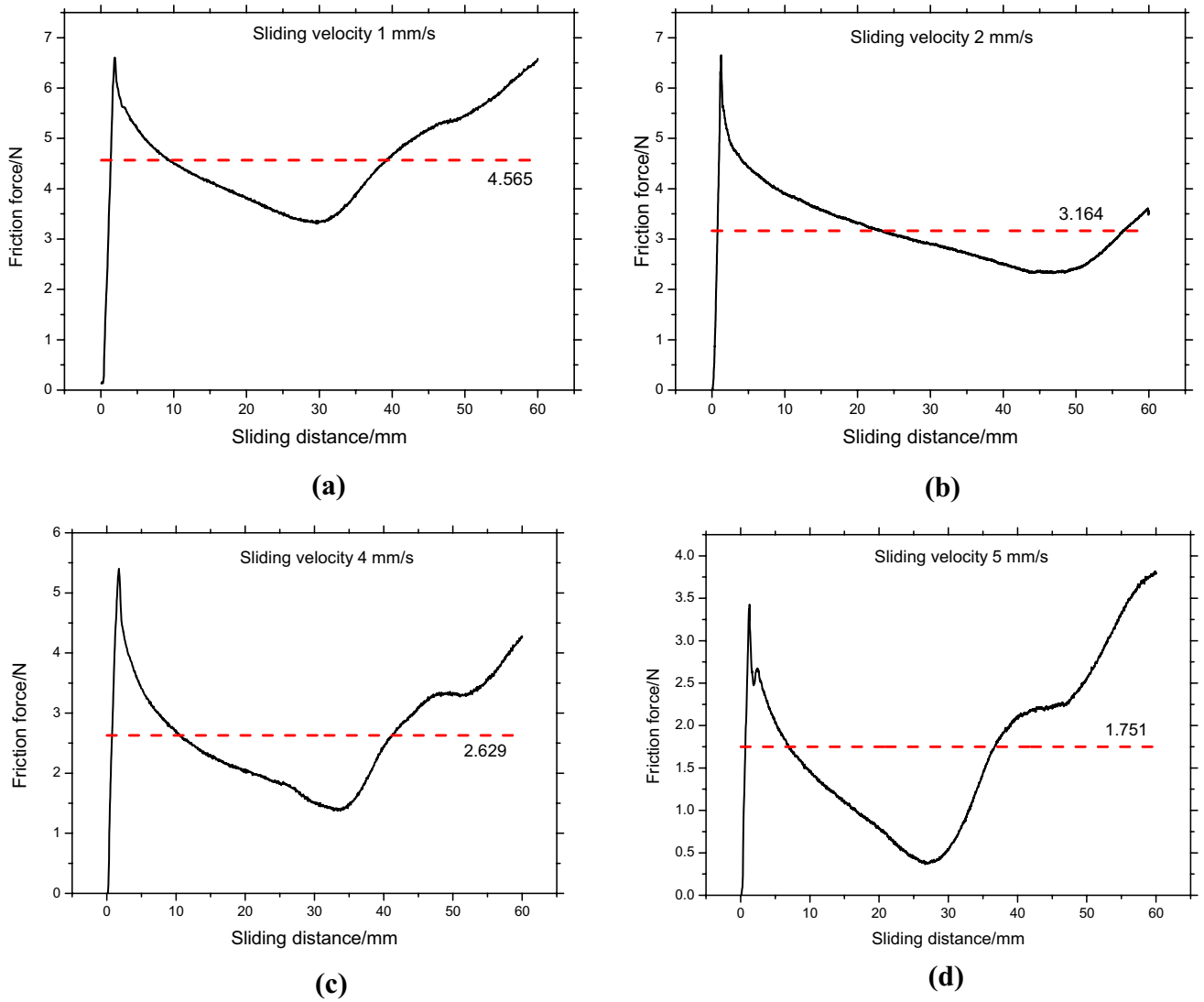

Fig. 12 Variation of the friction force with sliding distance under different sliding velocity. **a** 1 mm/s, **b** 2 mm/s, **c** 4 mm/s, and **d** 5 mm/s

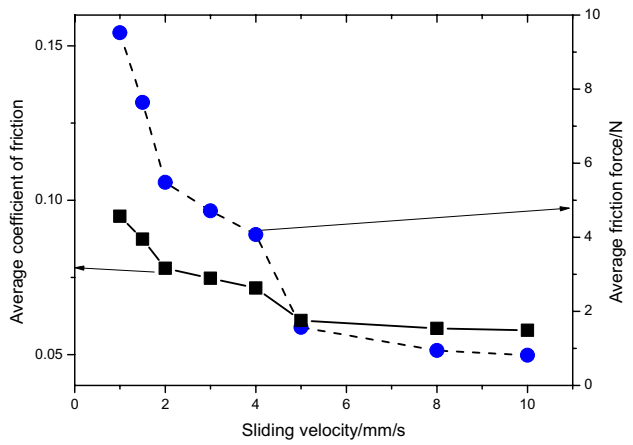

Fig. 13 Variation of average friction force and average friction coefficient with sliding velocity

with diameters ranging from 25.6 to 38.4 μm. Similar to those in the experimental test, the diameters of all particles are uniformly distributed, and the average diameter size is 30 μm.

The material properties and surface characteristics of the upper plate, the lower plate and spherical particles are consistent with the experimental tests. At the same time, to reduce the number of particles in the numerical calculation to reduce the calculation time, periodic space is set up in the numerical model. *P* is the pressure load applied to the upper plate, and its value is consistent with that in the experimental test. *U* is the sliding velocity of the lower plate, and its value is 2 mm/s in this study. The reticular line structure in Fig. 9b–d is the force chain network of this particle flow lubrication system, which is formed by the contact forces between particles as well as by the contact forces between

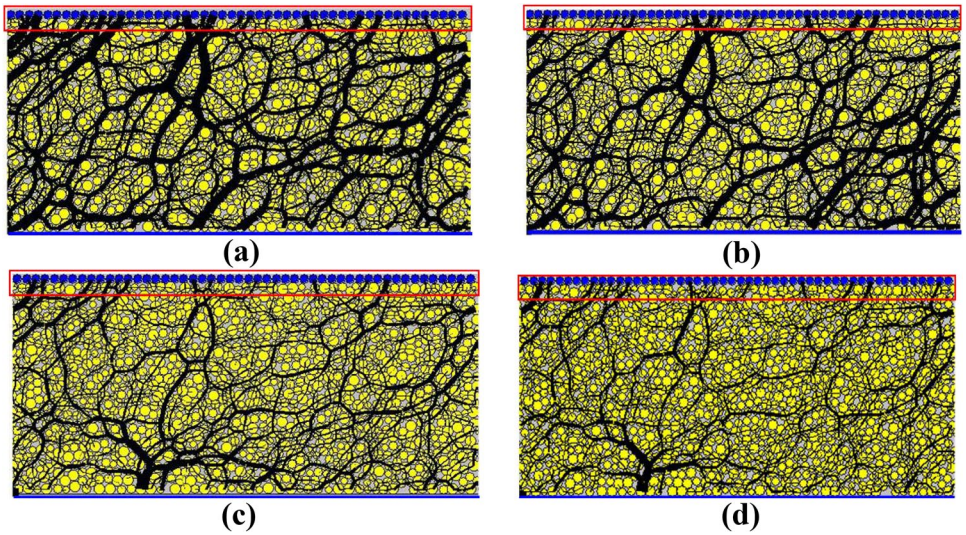

Fig. 14 The graph of force chain network between the upper plate and particle lubrication media under different sliding velocity. **a** 1 mm/s, **b** 2 mm/s, **c** 4 mm/s, and **d** 5 mm/s

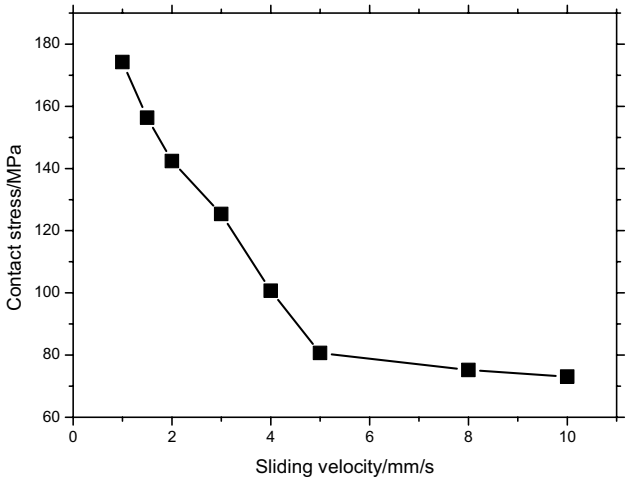

Fig. 15 Variation of contact stress with sliding velocity

particles and walls (the upper or lower plates). The thickness of the lines can directly reflect the magnitude of the contact force, and then influence the magnitude of the contact stress. It can be seen from Fig. 9b–d that the force chain line between the upper plate and the particle lubrication media becomes thicker with the increase of pressure load, indicating that the contact force and contact stress are increasing. Figure 10 shows the change law of contact stress with pressure load. It can be seen from the figure that the change trend of contact stress with pressure load is similar to that of the average coefficient of friction, which indicates that the change of contact stress directly influences the average coefficient of friction. The greater the contact stress is, the greater the average coefficient of friction will be.

3.3 The Influence of Sliding Velocity on Sliding Friction

Figures 11 and 12 show the variation of coefficient of friction and friction force with a sliding velocity between the upper plate and the particle lubricating media, respectively. The average coefficient of friction and average friction force are indicated by dotted lines in the figure, and the values are given on the right side of the figures. During the measurement, the pressure load applied to the upper plate is 37,500 N /m^2, the sliding velocity of the lower plate is 1, 1.5, 2, 3, 4, 5, 8 and 10 mm/s respectively, and the sliding distance of the lower plate is 60 mm. In order to ensure the accuracy of the measurement results, the test is repeated 10 times under the same sliding velocity, and each data point in the graph is the average value of the 10 measurement results.

It can be seen from Figs. 11 and 12 that the coefficient of friction and friction force increase rapidly to a certain peak value and then gradually decrease to the minimum value with the increase of sliding distance, and then show a trend of gradual increase with the increase of sliding distance. When the sliding velocity is 1, 2, 4 and 5 mm/s, the values of the average coefficient of friction are 0.154, 0.106, 0.089 and 0.059, and the values of corresponding average friction are 4.565, 3.164, 2.629 and 1.751 N, respectively. Figure 13 shows the variation law of average coefficient of friction and average friction force with sliding velocity.

As shown in Fig. 13, the average coefficient of friction and average friction force decrease with the increase of sliding velocity. The reason for this phenomenon is closely related to the change of force chain and contact stress with sliding velocity. Figure 14 shows the variation law of the force chain network of the particle flow lubrication system with the sliding velocity. The force chain line between the upper plate and the particle lubrication media becomes

thinner with the increase of the sliding velocity, indicating that the contact force and contact stress are decreasing. Figure 15 shows the variation law of contact stress with sliding velocity. It can be seen from this figure that the change trend of contact stress with sliding velocity is similar to that of the average coefficient of friction, and the contact stress decreases with the increase of sliding velocity, which indicates that the change of contact stress directly influences the magnitude of the average coefficient of friction. The result shows that the smaller the contact stress, the smaller the average coefficient of friction.

Furthermore, it can be seen from Figs. 13 and 15 that when the sliding velocity increases from 1 to 5 mm/s, the average coefficient of friction, average friction force and contact stress decrease greatly with the increase of sliding velocity. However, when the sliding velocity increases further, the average coefficient of friction, average friction force and contact stress also decrease with the increase of sliding velocity, but the decreasing range becomes very small. The reason for this change is that when the sliding velocity increases from 1 to 10 mm/s, the dynamic behavior of particles changes from the state of quasi-static flow to slow flow [36]. When the sliding velocity increases from 1 to 5 mm/s, the dynamic behavior of particles can be classified as quasi-static flow. In this state, the strength of the force chain between particles is larger and relatively stable.

Meanwhile, with the increase of sliding velocity, the strength of the force chain will be greatly reduced. When the sliding speed increases to 8–10 mm/s, the dynamic behavior of particles can be classified as the state of slow flow. In this state, the flow state of particles is much faster than that of quasi-static flow, the contact time between particles is relatively short, and the strength of the force chain between particles has been reduced to a lower level. Meanwhile, compared with the quasi-static flow state, the decreasing range of the strength of the force chain becomes smaller with the increase of the sliding velocity.

4 Conclusions

In this study, a self-developed experimental system was designed to investigate the friction behaviors of the parallel plates under dry particle lubrication.

The sliding tribological behavior of particle flow lubrication is closely related to the measurement of the maximum contact stress between the upper plate and the single particle. Meantime, the change of the maximum contact stress can be reflected by the force chain network. By experimental comparison, dry particle lubrication behaves excellent lubricity on sliding friction.

The force chain line between the upper plate and the particle lubrication media becomes thicker with the increase of pressure load, indicating that the contact force and contact stress are increasing. These are the reasons for the following experimental results: the average coefficient of friction between the upper palate and particles increases rapidly with the increase of pressure load, while the average friction force increases linearly with the increase of pressure load.

The average coefficient of friction and average friction force decrease with the increase of sliding velocity. The reason for this phenomenon is also closely related to the change of force chain and contact stress with sliding velocity. The force chain line between the upper plate and the particle lubrication media becomes thinner with the increase of the sliding velocity, indicating that the contact force and contact stress are decreasing. The greater the contact stress is, the greater the average coefficient of friction will be.

The current experimental work provides useful information for understanding the sliding tribological behavior of particle flow lubrication. Meantime, it is an important step to study the influence of external conditions (i.e., velocity, load) on the sliding tribological characteristics of particle flow lubrication, which can provide guidance and theoretical support for the selection of die parameters under the condition of particle lubrication in warm forming die manufacturing.

Acknowledgements This work was supported by the National Natural Science Foundation of China (51605150). This work was also partly supported by the Henan Provincial Key Teacher Training Program (2019GGJS265), the Scientific and Technological Research Projects in Henan Province (212102210432), and the Key Scientific Research Projects of Henan Universities (21A110007 and 21A130001)

References

1. Xu, J., Chen, R., Hong, H., Yuan, X., Zhang, C.: Static characteristics of high-temperature superconductor and hydrodynamic fluid-Film compound bearing for rocket engine. IEEE Trans. Appl. Supercond. **25**(6), 1–8 (2015)
2. Zhu, S., Cheng, J., Qiao, Z., Yang, J.: High temperature solid-lubricating materials: a review. Tribol. Int. **133**, 206–223 (2019)
3. Su, Y., Hu, T., Fan, H., Song, J., Zhang, Y.: Surface engineering design of alumina/molybdenum fibrous monolithic ceramic to achieve excellent lubrication in a high vacuum environment. Tribol. Lett. **66**(2), 72 (2018)
4. Pettersson, U., Jacobson, S.: Textured surfaces for improved lubrication at high pressure and low sliding speed of roller/piston in hydraulic motors. Tribol. Int. **40**, 355–359 (2007)
5. Wornyoh, E.Y.A., Jasti, V.K., Higgs, C.F.: A review of dry particulate lubrication: Powder and granular materials. J. Tribol. **129**(2), 1345–1360 (2007)
6. Wang, W., Kong, J., Gu, W., Liu, K.: Experimental study on macro and micro characteristics of powder lubricant layer in frictional warm interface. Tribology **36**(2), 233–239 (2016)
7. Meng, F., Pang, M., Liu, K.: Constitutive relation and mechanical mechanism analysis in granular lubrication. Ind. Lubr. Tribol. **72**(5), 621–628 (2019)

8. Wang, C., Wang, W., Liu, Y., Liu, K.: Micro morphological observation and mechanism analysis of boundary layer evolution in mixed powder lubrication. Lubr. Sci. **30**(3), 91–101 (2018)
9. Wang, W., Liu, Y., Zhu, G., Liu, K.: Using FEM–DEM coupling method to study three-body friction behavior. Wear **318**(1–2), 114–123 (2014)
10. Hentschel, H.G.E., Procaccia, I., Roy, S.: Diffusion in agitated frictional granular matter near the jamming transition. Phys. Rev. E **100**(4), 042902 (2019)
11. Ness, C., Mari, R., Cates, M.E.: Shaken and stirred: random organization reduces viscosity and dissipation in granular suspensions. Sci. Adv. **4**, 3296 (2018)
12. Heshmat, H., Walton, J.F.: High-temperature powder-lubricated dampers for gas-turbine engines. J. Propul. Power **8**(2), 449–456 (1992)
13. Meng, F.J., Liu, K., Wang, W.: The force chains and dynamic states of granular flow lubrication. Tribol. Trans. **58**(1), 70–78 (2015)
14. Yang, B., Wang, W., Liu, K., Liu, Y.: Observation and analysis of micro-behavior characteristics and element contents during boundary layer evolution under powder particulate lubrication. Tribol. Lett. **64**(1), 2 (2016)
15. Iordanoff, I., Berthier, Y., Descartes, S., Heshmat, H.: A review of recent approaches for modeling solidthird bodies. J. Tribol. **124**(4), 725–735 (2002)
16. Heshmat, H.: The quasi-hydrodynamic mechanism of powder lubrication: Part 2: lubricant film pressure profile. Lubr. Eng. **48**(5), 373–383 (1992)
17. Heshmat, H., Brewe, D.E.: Performance of a powder lubricated-journal bearing with ws2 powder: experimental study. J. Tribol. **118**(3), 484–491 (1996)
18. Elkholy, K.N., Khonsari, M.M.: Granular collision lubrication: experimental investigation and comparison to theory. J. Tribol. **129**(4), 923–932 (2007)
19. Elkholy, K.N., Khonsari, M.M.: Experimental investigation on the stick–Slip phenomenon in granular collision lubrication. J. Tribol. **130**(2), 021302 (2008)
20. Reddy, N.S.K., Rao, P.V.: Experimental investigation to study the effect of solid lubricants on cutting forces and surface quality in end milling. Int. J. Mach. Tools Manuf. **46**(2), 189–198 (2006)
21. Gopal, A.V., Rao, P.V.: Performance improvement of grinding of sic using graphite as a solid lubricant. Mater. Manuf. Process **19**(2), 177–186 (2004)
22. Iordanoff, I., Elkholy, K., Khonsari, M.M.: Effect of particle size-dispersion on granular lubrication regimes. Proc. IME J. **222**(6), 725–739 (2008)
23. Kimura, R., Yoshida, M., Sasaki, G., Pan, J., Fukunaga, H.: Characterization of heat insulating and lubricating ability of powder lubricants for clean and high quality die casting. J. Mater. Process Technol. **130**, 289–293 (2002)
24. Wang, W., Gu, W., Liu, K., Wang, F., DEM Tang, Z.: simulation on the startup dynamic process of a plain journal bearing lubricated by granular media. Tribol. Trans. **57**(2), 198–205 (2014)
25. Meng, F., Liu, K., Tang, Z., Wang, W., Liu, X.: Multiscale mechanical research in a dense granular system between sheared parallel plates. Phys. Scripta **89**(10), 105702 (2014)
26. Yan, X., Wang, W., Liu, X., Zhu, G.: Using a coupled FEM-DEM method to study the nonlinear phenomena of third-body behavior. Proc. IME. J. **208–210**, 1–14 (2020)
27. Xun, T., Wang, X., Liu, K., Wang, Z., Wei, D.: Characteristics of force chains in frictional interface during abrasive flow machining based on discrete element method. Adv. Manuf. **6**, 355–375 (2018)
28. Chattoraj, J., Gendelman, O., Ciamarra, M.P., Procaccia, I.: Oscillatory instabilities in frictional granular matter. Phys. Rev. Lett. **123**, 098003 (2019)
29. Lim, M.X., Souslov, A., Vitelli, V., Jaeger, H.M.: Cluster formation by acoustic forces and active fluctuations in levitated granular matter. Nat. Phys. **15**(5), 460–464 (2019)
30. Zhang, H., Liu, S., Xiao, H.: Sliding friction of shale rock on dry quartz sand particles. Friction **7**(4), 307–315 (2019)
31. Walker, D.M., Tordesillas, A., Kuhn, M.R.: Spatial connectivity of force chains in a simple shear 3D simulation exhibiting shear bands. J. Eng. Mech. **143**, C4016009 (2016)
32. Gendelman, O., Pollack, Y.G., Procaccia, I., Sengupta, S., Zyiberg, J.: Whatdetermines the static force chains in stressed granular media? Phys. Rev. Lett. (2016). https://doi.org/10.1103/PhysRevLett.116.078001
33. Lu, X., Khonsari, M.M.: On the lift-off speed in journal bearings. Tribol. Lett. **20**(3–4), 299–305 (2005)
34. Yu, C., Tichy, J.: Granular collision lubrication: effect of surface roughness, particle size and solid fraction. Tribol. Trans. **39**(3), 537–546 (1996)
35. Sawyer, W.G., Tichy, J.: Lubrication with grain flow: continuum theory, particle simulations, comparison with experiment. J. Tribol. **123**(4), 777–784 (2001)
36. Campbell, C.S.: Granular material flows—An overview. Powder Technol. **162**, 208–229 (2006)